The Journal of Navigation (2024), **77**:2 257–275
doi:10.1017/S0373463324000304

CAMBRIDGE UNIVERSITY PRESS

RESEARCH ARTICLE

Performance of GNSS space service for geostationary autonomous operations

Fangtan Jiao,[1,2,3,4]* Yuxin Hu,[1,2,3] and Xiaodong Yu[1,2]

[1] Aerospace Information Research Institute, Chinese Academy of Sciences, Beijing 100094, China
[2] Key Laboratory of Geo-spatial Information Processing and Application System Technology, Chinese Academy of Sciences, Beijing 100190, China
[3] University of Chinese Academy of Sciences, Beijing 100049, China
[4] School of Electronic, Electrical and Communication Engineering, University of Chinese Academy of Sciences, Beijing 100049, China.
*Corresponding author: Fangtan Jiao; Email: jiaofangtan22@mails.ucas.ac.cn

Received: 9 February 2024; **Revised:** 6 June 2024; **Accepted:** 13 August 2024; **First published online:** 3 December 2024

Keywords: BDS; GNSS; onboard autonomous orbit determination

Abstract

The geostationary orbit (GEO) belt hosts a substantial number of high-value satellites, making the study of autonomous navigation within this area significant. Features of autonomous operations such as patrolling the GEO belt and frequent manoeuvres at a certain location make real-time positioning using the Global Navigation Satellite System (GNSS) valuable. This paper studies the performance of positioning with GNSS considering main lobe and side lobe signals at different longitudes in the GEO belt. The research delves into the visibility and Position Dilution of Precision (PDOP) across the GEO belt, analysing the performance of the Global Positioning System (GPS), GLObalnaya NAvigatsionnaya Sputnikovaya Sistema (GLONASS) in Russian, BeiDou Navigation Satellite System (BDS), Galileo Navigation Satellite System (Galileo) and multi-systems. In particular, this paper investigates the impact of asymmetric constellations of mixed GEO, Inclined Geosynchronous Orbit (IGSO) and Medium Earth Orbit (MEO) satellites. The study reveals that BDS hybrid constellation provides long-term stable signal coverage over the GEO space above North America and Atlantic Ocean, where GEO signals are more sustainable while IGSO signals have wider coverage. This advantage positions BDS favourably in terms of performance in these regions.

1. Introduction

Geostationary orbit satellites play a crucial role in various domains, including communications, earth observation and navigation. Since the launch of the first GEO satellite, SYNCOM3, in 1964, hundreds of GEO satellites have been launched to date (CFSCC, 2023). As of 2023, there are approximately 500 operational GEO satellites (UCS, 2023). Moreover, administrators have declared over 3000 GEO positions to the International Telecommunication Union (ITU). The extensive use of GEO has resulted in a large number of high-value satellites operating in this region. In pursuit of obtaining more details regarding the operation and health status of satellites, and aiming for more effective maintenance of these targets, GEO operations, including on-orbit services, have garnered significant attention (Xu et al., 2011). GEO on-orbit servicing satellites usually must continuously patrol the GEO belt to observe and update the status of high-value satellites. For example, they may approach an anomalous satellite, then move around to gather information and analyse the anomaly, such as observing target structures and assessing the damage caused by micrometeoroids or sub-centimetre space debris. Currently, systematic tests of moving around and inspection have been conducted by the United States. The Micro-satellite

© The Author(s), 2024. Published by Cambridge University Press on behalf of The Royal Institute of Navigation

https://doi.org/10.1017/S0373463324000304 Published online by Cambridge University Press

Technology Experiment (MiTEx) came close to approximately 100 km and inspected the disabled Defense Support Program-23 satellite (DSP-23) in 2009. The USA 253 satellite and its series, launched in batches in 2014, 2016 and 2022, conducted patrols in the GEO belt and closely inspected several satellites through moving around, achieving centimetre-level imaging at a distance of approximately 10 km (Weeden and Samson, 2018).

Many existing tracking methods for GEO satellites, such as angle measurement techniques, Very Long Baseline Interferometry (VLBI) and connected-element interferometry (CEI), exhibit a significant reliance on ground stations (Du, 2006). Given that GEO on-orbit servicing satellites must constantly patrol the GEO belt and considering China's lack of ground stations worldwide, these satellites cannot operate over space beyond China. In contrast, space-based GNSS offers a global, all-weather and continuous solution. Being independent of territorial boundaries, it can effectively enhance the real-time navigation capability of GEO satellites when ground stations are not visible. In addition, on-orbit servicing satellites require a prompt response to complicated and changing situations, as well as ongoing trajectory planning during a mission (Maestrini and Di Lizia, 2022), which places high autonomy requirements on the satellite's guidance, navigation and control (GNC) system. Alternatively, traditional methods usually involve extensive human intervention, posing challenges in attaining optimal planning and falling short of effectively meeting the real-time and autonomy requirements for more complex tasks (Woffinden and Geller, 2007). Therefore, autonomous operations are critical, receiving heightened emphasis from NASA as a key technology for space missions in the next generation (Starek et al., 2016). As an important part of the GNC system, autonomous navigation and real-time positioning capability with higher accuracy can effectively improve the trajectory planning effect of satellites. GNSS-based autonomous navigation systems not only liberate themselves from the constraints of ground stations but also offer substantial benefits, including minimal error accumulation, cost-effectiveness and high real-time positioning accuracy. This stands in stark contrast to conventional autonomous navigation systems such as inertial and visual navigation. These advantages greatly facilitate the implementation of autonomous operations in the GEO belt.

The use of GNSS to provide precise orbit determination and navigation for satellites has been widely applied to low earth orbit (LEO) satellites (Bock et al., 2002; Kang et al., 2006; Li et al., 2017; Zhao et al., 2020). In the 1980s, the concept of using GPS to provide navigation services for GEO satellites was introduced (Ananda and Jorgensen, 1985). In 2006, Bauer et al. (2006) formalised the concept of a Space Service Volume (SSV), indicating that navigation satellites, in addition to serving the Terrestrial Service Volume (TSV) up to 3,000 km, were also required to serve medium-orbit and high-orbit spacecraft operating between 3,000 km and 36,000 km. In recent years, research and initiatives on SSV have become a hot topic in the field of high-orbit satellite navigation (Bauer et al., 2017). In 2018, Working Group B of the International Committee on GNSS (ICG) released the SSV booklet, which lists the characteristics of each navigation constellation, such as pseudo-range accuracy, received signal power and signal availability. It also illustrates that the ability of a multi-constellation outperforms any individual constellation (UNOOSA, 2021). Because the centre of the navigation signal points towards the centre of the earth, GEO satellites can only receive unobstructed signals from the other side of the earth. This characteristic results in a significant degradation of GNSS signal availability, given its specific application environment (Winternitz et al., 2009). Shi et al. (2021) assumed several satellites operating at fixed GEO longitudes and investigated the navigation effects in the case of combining the GPS, BDS, Galileo and GLONASS constellations. The result indicated that effective service to GEO is not attainable by solely considering the main lobe signal. Furthermore, the design of a high-sensitivity receiver to realise the reception of the side lobe signal can be more effective in improving the effect of GEO autonomous navigation (Jing et al., 2015). In 2011, the Space-Based Infrared System GEOstationary-1 (SBIRS GEO-1) was launched and equipped with a dual-frequency GPS receiver, realising onboard real-time navigation and analysing GPS L1 antenna group delay as seen from large angles off the beam centre (Barker and Frey, 2012). In 2016, Geostationary Operational Environmental Satellite-R (GOES-R) was launched and equipped with a General Dynamics' Viceroy-4 GPS space-borne receiver (Wang et al., 2020). The test results of GOES-R, considering both main lobe and side lobe

https://doi.org/10.1017/S0373463324000304 Published online by Cambridge University Press

signals, showed that the average number of visible navigation satellites was up to 11 and the position accuracy was better than 30 m (Winkler et al., 2017). In 2017, Chinese Tongxin Jishu Shiyan-2 (TJS-2) carried a GNSS-compatible receiver, capable of receiving main lobe and side lobe signals, and achieved 27-metre positional accuracy in orbit (Jiang et al., 2018).

Autonomous navigation for GEO satellites based on GNSS considering side lobe signals has important research value and application (Ashman et al., 2018). Early GEO satellite navigation and orbit determination studies that considered side lobe signals were mainly based on GPS or a combination of GPS, Galileo and GLONASS (Qin and Liang, 2008; Filippi et al., 2010; Lorga et al., 2010; Marmet et al., 2015). During the period of the above studies, the BDS was a regional system. Thus, there were many areas where GEO users could not achieve single epoch positioning using only BDS, even considering the side lobe signal. In July 2020, the construction of the BDS global system was completed, and the research on BDS-based autonomous navigation for GEO users became more promising. Lin et al. (2020) studied the effects of BDS side lobe signals for navigation of a hypothetical GEO satellite at a specific longitude. Wang et al. (2021) used the measured data of TJS-2 and demonstrated that the reception of the side lobe signal from navigation satellites can effectively improve the overall navigation performance of GEO satellites. Guan et al. (2022) studied the effectiveness of GEO satellite navigation comparing and combining the use of GPS, BDS, Galileo and GLONASS, demonstrating the visibility advantages of BDS. Others are user-oriented, investigating receiver design for different signal regimes and onboard signal processing methods based on specific tasks (Wang et al., 2011; Capuano et al., 2017; Zou et al., 2019; Yang et al., 2021). All the studies mentioned above are analyses of GNSS space service for real or hypothetical GEO missions operating at a fixed longitude. Thus, there is a lack of analysis of GNSS signal visibility and PDOP across the GEO belt for on-orbit servicing satellites that constantly patrol the GEO belt and perform at different longitudes. In addition, all the other global systems have symmetric constellations except BDS, and the hybrid constellation of BDS could provide better service for areas covered by GEO/IGSO satellite signals (Wang et al., 2019). Therefore, due to the characteristics of moving status for GEO on-orbit servicing missions, an asymmetric constellation of BDS could affect the performance of space service in the GEO belt which needs to be investigated.

In this paper, we will explore the impact of incorporating both the main lobe and side lobe signals on real-time navigation across the entire GEO belt. Considering the BDS constellation of mixed MEO/GEO/IGSO satellites, we will also study the effect of asymmetric constellations on different GEO regions in terms of visibility and PDOP. Moreover, due to the differences in the contributions of the different types of satellites in the hybrid constellation (Meng et al., 2020), the characteristics of GEO and IGSO satellites will also be investigated separately in this paper. It is worth noting that measured data of GNSS precise ephemeris from the International GNSS Monitoring and Assessment System (iGMAS) and transmitter signal patterns considering SSV will be used in this study. Furthermore, the reasonableness of experimental results in this paper will be validated by results from GOES-R (Winkler et al., 2017), TJS-2 (Wang et al., 2021) and Japanese Data Relay System-1 (JDRS-1) (Nakajima et al., 2023). Additionally, the study will address the autonomous navigation capabilities of GEO users during exceptional circumstances using only BDS. Furthermore, the analysis will delve into the advantages offered by BDS GEO and IGSO satellites in augmenting autonomous navigation performance within the GEO belt when compared with relying solely on GPS.

2. Experimental principle

2.1. Visibility of single navigation satellite

For a single navigation satellite, visibility is the first step in assessing its navigational performance. For GNSS satellites, the earth coverage beam is applied for the design of spatial filtering. Therefore, antennae of ground and LEO users usually point in the zenith direction to receive navigation signals. However, it is not feasible for GEO users, because they can only receive unobstructed navigation signals

https://doi.org/10.1017/S0373463324000304 Published online by Cambridge University Press

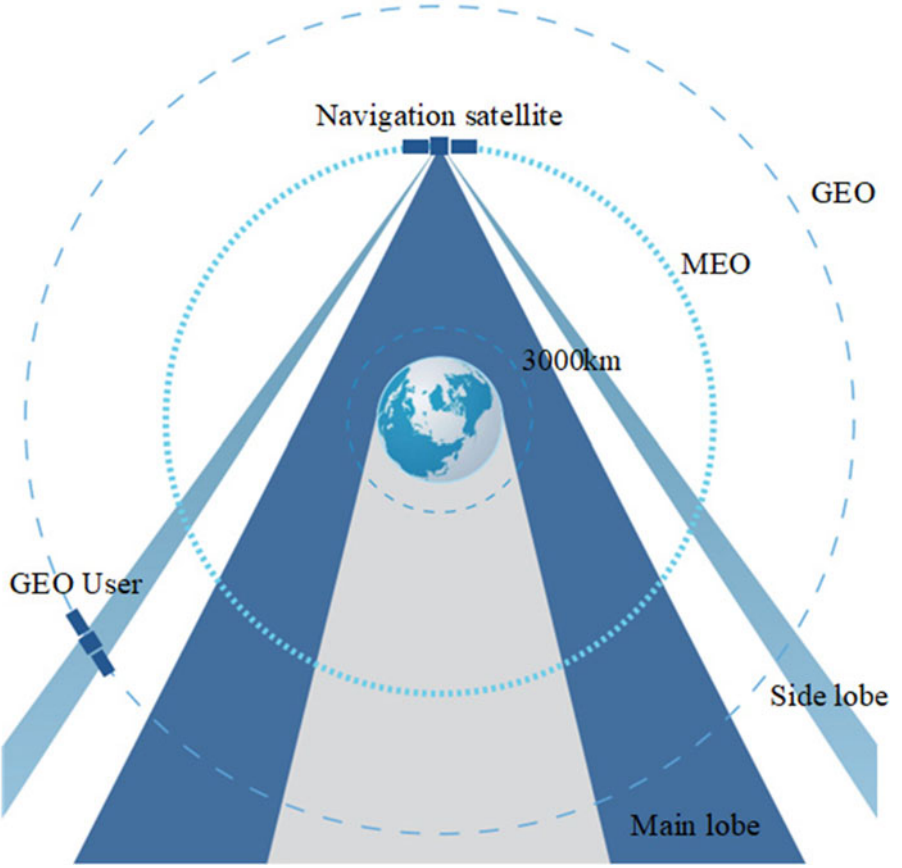


Figure 1. *Schematic diagram of GNSS signal propagation.*

from the opposite side of the earth. In addition, the high-sensitivity receiver enables the GEO satellite to receive the side lobe signal from the navigation satellite, as shown in Figure 1.

Analysing the visibility of the navigation satellite signal requires modelling the propagation link as follows (Chai et al., 2018):

$$P_R = P_T + G_T + 20\lg(c/4\pi df) + L_A + G_R \tag{1}$$

where P_R is the received power, P_T is the transmit power, G_T is the transmit gain, the sum of P_T and G_T is the Effective Isotropic Radiated Power (EIRP), $20\lg(c/4\pi df)$ is the free-space propagation loss, $c = 299{,}792{,}458$ m/s is the speed of light, d is the distance between the transmitter and the receiver, f is the carrier frequency of the signal, L_A is the atmospheric loss, and G_R is the receiver gain. Moreover, when the signal is obscured by the earth, it is considered to be invisible.

For the receiving terminal, the carrier-to-noise ratio C/N_0 is a key measure of whether the signal can be received, shown as

$$C/N_0 = P_R - 10\lg(kT) \tag{2}$$

where $k = 1{\cdot}38 \times 10^{-23}$ J/K is the Boltzmann constant and T is the ambient temperature.

When the carrier-to-noise ratio is greater than the reception threshold, the GNSS signal can be received, and considered as visible. Since the proportion of signal subjected to atmospheric losses is slight, this item is ignored. Therefore, the visibility of navigation satellites is related to the transmitter design with key elements P_T, G_T and f, the position vector of GEO satellites with respect to the

https://doi.org/10.1017/S0373463324000304 Published online by Cambridge University Press

Table 1. *GNSS design parameters.*

Constellation	GPS	GLONASS	BDS		Galileo
			MEO	GEO/IGSO	
Signal name	L1 C/A	L1	B1C	B1I	E1 B/C
Signal centre frequency (MHz)	1,575·42	1,605·375[a]	1,575·42	1,561·098	1,575·42
Received power using a 0 dBi right-hand circular polarised antenna at GEO (dBW)	−184·0	−179·0	−184·2	−185·9	−182·5
Main lobe reference off-boresight angle (°)	23·5	26	25	19	20·5
Reference angle range with a 25 dB lower reception threshold (°)	[0, 60]	[0, 60][b]	[0, 60]	[0, 23]∪[29, 35]	[0, 60][c]

[a]The GLONASS signal is related to the satellite Pseudo-Random Noise (PRN) and the model is set uniformly according to the data in the booklet.
[b,c]The publicly available information on GLONASS and Galileo is not comprehensive, so parameters assumed in the model are consistent with GPS to simplify the calculations.

navigation satellite with key element d and P_R in this direction, the receiver design with key element G_R, and the reception threshold.

In addition, the ephemeris error of a navigation satellite also affects the positioning of GEO satellites, but since this error is agreed upon by the GNSS service performance specification, it is not analysed as a focus in this paper.

2.2. Visibility of GNSS constellations

An important metric for assessing the navigation performance of GNSS constellations is the number of visible satellites. Real-time navigation solving is only possible when the number of visible navigation satellites is not less than 4 for a single epoch positioning, so a larger number of visible satellites is the basis for realising effective autonomous navigation. Since the visibility is affected by both the transmitter and receiver sides, the design will take into account the signal pattern, free space propagation loss, minimum received civilian signal power at GEO and link margin to give a range of the off-boresight angle as a unified standard. Specific parameters from ICG's SSV booklet are shown in Table 1 (UNOOSA, 2021).

Since the reception of the main lobe signal is not sufficient for navigation, the use of the side lobe signal needs to be considered. If the current reception threshold is lowered by 25 dB as a new criterion, GPS can achieve visibility within a 60° off-boresight angle as a calculated result from the propagation link model in this paper and the data of GPS transmitters' antenna gain patterns (Marquis and Reigh, 2015). Meanwhile, the design of the BDS transmitter for the next generation considering SSV is also 60°, but BDS GEO/IGSO satellites do not have the plan of SSV enhancement, so the design of the existing regime achieves only 23° for the main lobe and 29° to 35° for the side lobe for this requirement. In particular, the publicly available information on GLONASS and Galileo is not comprehensive compared with GPS, so the parameters assumed in the model are consistent with GPS to simplify the calculations. In summary, it can be assumed that navigation satellites are oriented towards the Earth, which means the z-axis of the body-fixed frame (the unit vector of antenna pointing) is directed to the centre of the Earth. Then a unit vector of the navigation satellite pointing towards the GEO user can be defined as $\boldsymbol{e}$. It is considered to be visible when both of the following two conditions are met. One is that the link

https://doi.org/10.1017/S0373463324000304 Published online by Cambridge University Press

between the navigation satellite and the GEO user is not blocked by the Earth, and the other is that the angle θ between $\boldsymbol{e}$ and the z-axis is in the range of the main lobe or side lobe of the signal. The number of visible satellites n_{visible} is calculated as

$$n_{\text{visible}} = \sum_{\alpha \in C} \sum_{i=1}^{n_\alpha} \text{bool}\left(f_\alpha \left(\cos^{-1}\left(\begin{bmatrix} 0 \\ 0 \\ 1 \end{bmatrix}^{\text{T}} \frac{(\boldsymbol{q}_{\text{BI},i}^{\alpha} \times \boldsymbol{q}_{\text{EI}}^{-1}) \otimes (\boldsymbol{R} - \boldsymbol{r}_i^{\alpha})}{||(\boldsymbol{q}_{\text{BI},i}^{\alpha} \times \boldsymbol{q}_{\text{EI}}^{-1}) \otimes (\boldsymbol{R} - \boldsymbol{r}_i^{\alpha})||_2} \right), ||\boldsymbol{r}_i^{\alpha}||_2 \right) \right) \tag{3}$$

where C represents the set of GNSS constellations included in the calculation and n_α represents the number of satellites in constellation α. Here, $\boldsymbol{q}_{\text{EI}}$ is the quaternion expressing the orientation of the Earth-centred, Earth-fixed coordinate system (ECEF) with respect to the inertial frame and $\boldsymbol{q}_{\text{BI},i}^{\alpha}$ is the quaternion expressing the orientation of the body-fixed frame of the ith navigation satellite in constellation α with respect to the inertial frame. Additionally, $\otimes$ is the operator that rotates a vector by a quaternion and $\times$ is quaternion multiplication. Furthermore, $\boldsymbol{R}$ and $\boldsymbol{r}_i^{\alpha}$ are vectors of the GEO satellite and the ith navigation satellite in constellation α in the ECEF reference system, respectively. Here, $\text{bool}(f_\alpha(\theta, r))$ is a function of angle θ and the geocentric distance r of the navigation satellite in constellation α, and this function is used to determine the visibility of the navigation satellite. When the value of $f_\alpha(\theta, r)$ is non-zero, the result of $\text{bool}(f_\alpha(\theta, r))$ is 1 (true), regarded as visible. When the value of $f_\alpha(\theta, r)$ is zero, the result of $\text{bool}(f_\alpha(\theta, r))$ is 0 (false), regarded as invisible. Moreover, the expression for $f_\alpha(\theta, r)$ is

$$\begin{aligned} f_\alpha(\theta, r) = \text{sgn}\left(\theta - \sin^{-1}\frac{r_{\text{earth}} + h_{\text{iono}}}{r}\right) - \text{sgn}(\theta - \varphi_{\text{main}}^{\alpha}) \\ + \sum_{k=1}^{n_{\text{side}}^{\alpha}} (\text{sgn}(\theta - \inf\{\psi \in \mathcal{S}_k^{\alpha}\}) - \text{sgn}(\theta - \sup\{\psi \in \mathcal{S}_k^{\alpha}\})) \end{aligned} \tag{4}$$

where $r_{\text{earth}} = 6{,}378{\cdot}14\,\text{km}$ represents the radius of the earth. In particular, taking into account that the ionosphere greatly affects positioning accuracy and that the high-density zone is located within $h_{\text{iono}} = 350\,\text{km}$ above the earth's surface (Zeng et al., 2004), signals crossing within this range are considered unavailable. Here, $\varphi_{\text{main}}^{\alpha}$ represents the main lobe off-boresight angle for satellites of constellation α at a set threshold and $\mathcal{S}_k^{\alpha}$ represents the set of angles for the kth out of a total of n_{side}^{α} visible side lobes for that type of satellite.

2.3. PDOP of GNSS constellation

After determining the number of visible satellites, the dilution of precision can be calculated. This parameter is another important evaluation metric that describes the amount of amplification from the User Equivalent Range Error (UERE) to the user navigation error. Since measurement errors cannot be avoided in practical applications, and are related to the conditions of both the space segment and the receiver status, the dilution of precision should be minimised for the GNSS constellation to improve the overall positioning accuracy. This paper focuses on analysing the Position Dilution of Precision (PDOP), which quantifies the effect of the geometric distribution of visible GNSS constellations in three-dimensional space on navigation accuracy (3D position accuracy).

For ease of computation, the matrix $\boldsymbol{H}$ is first defined, which contains the unitised direction vector of the user with respect to all visible navigation satellites in the ECEF reference frame, as

$$\boldsymbol{H} = \begin{bmatrix} \dfrac{\boldsymbol{R} - \boldsymbol{r}_1^{v}}{||\boldsymbol{R} - \boldsymbol{r}_1^{v}||_2} & \cdots & \dfrac{\boldsymbol{R} - \boldsymbol{r}_j^{v}}{||\boldsymbol{R} - \boldsymbol{r}_j^{v}||_2} & \cdots & \dfrac{\boldsymbol{R} - \boldsymbol{r}_{n_{\text{visible}}}^{v}}{||\boldsymbol{R} - \boldsymbol{r}_{n_{\text{visible}}}^{v}||_2} \end{bmatrix} \in \mathbb{R}^{3 \times n_{\text{visible}}} \tag{5}$$

where $\boldsymbol{r}_j^{v}$ is the position vector of the jth visible navigation satellite.

https://doi.org/10.1017/S0373463324000304 Published online by Cambridge University Press

Table 2. *GNSS constellation parameters.*

Constellation	Orbit type	Number of satellites
GPS	MEO	32 (in 6 planes)
GLONASS	MEO	21 (in 3 planes)
BDS	MEO	27 (in 3 planes)
	GEO	5
	IGSO	10
Galileo	MEO	25 (in 3 planes)

PDOP is calculated as shown below, following the derivations in UNOOSA (2021):

$$\mathrm{PDOP} = \sqrt{\mathrm{tr}\left(\left(\boldsymbol{H}\boldsymbol{H}^T - \frac{\boldsymbol{d}_s \boldsymbol{d}_s^T}{n_{\mathrm{visible}}}\right)^{-1}\right)} \tag{6}$$

where $\boldsymbol{d}_s$ is the sum of the unitised direction vectors of all visible navigation satellites relative to the user, whose expression is shown as

$$\boldsymbol{d}_s = \sum_{j=1}^{n_{\mathrm{visible}}} \frac{\boldsymbol{R} - \boldsymbol{r}_j^v}{||\boldsymbol{R} - \boldsymbol{r}_j^v||_2} \tag{7}$$

The size of PDOP depends only on the geometric distribution of the GNSS constellation with respect to the user, and is more suitable for evaluating the performance of different GNSS constellations and multi-constellations in providing services to the GEO space.

3. Experimental analysis

3.1. Data source

The ephemeris parameters for this study were obtained from the iGMAS. Considering the revisit time of BDS, which is the focus of this paper, is 7 days, the measured data of this length of time were selected to construct the GNSS constellation model. In this paper, the data from July 30, 2023, to August 5, 2023 (the 917th BeiDou week) were used as an example for calculation. The data for this period included satellites' position data of the GPS, GLONASS, BDS (including MEO, GEO and IGSO satellites) and Galileo constellations in the ECEF reference frame, as shown in Table 2. The precise ephemeris was sampled at 15-minute intervals and it should be noted that satellites in unhealthy states were excluded.

3.2. Visibility analysis

The analysis of the number of visible satellites for a single constellation is first considered, as shown in Figure 2. It is worth noting that the results of the single constellation in the figure consider both main lobe and side lobe signals, and the results considering only the main lobe signal are not shown in the figure because it is impossible for real-time single-point navigation all the time. Each system exhibits periodicity in the time dimension, since different satellites within a GNSS constellation have similar orbital periods, and the geometry of the constellation at a given moment in time is similar to that after one orbital period. In particular, the orbital frequencies ranked from lowest to highest are Galileo, BDS, GPS and GLONASS over the 7-day sampling period, which is coherent with the orbital altitudes of the MEO satellites of the four constellations, because higher orbital altitudes have longer orbital periods, which corresponds to lower frequencies of change.

https://doi.org/10.1017/S0373463324000304 Published online by Cambridge University Press

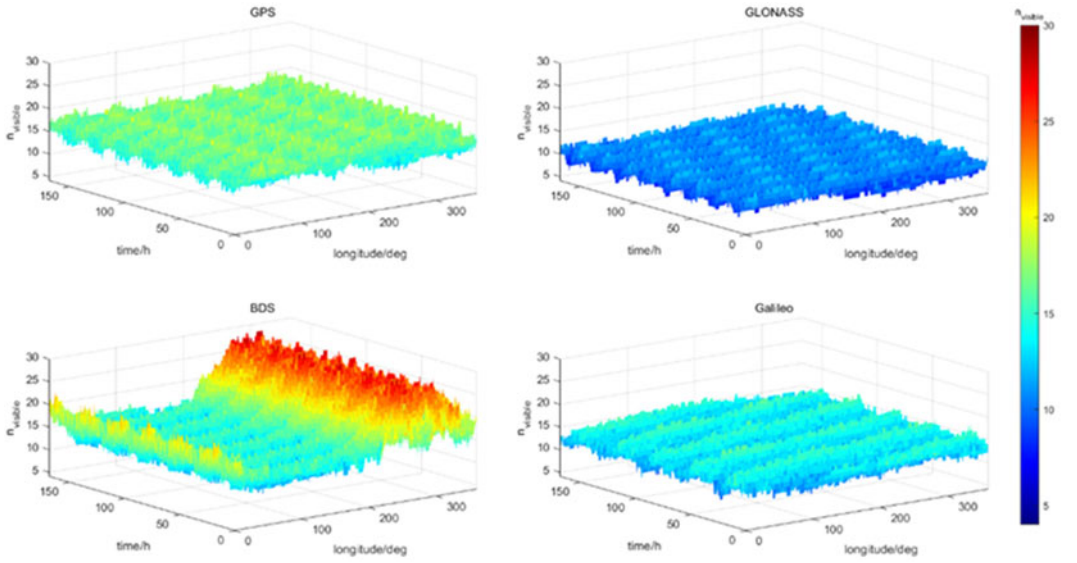


Figure 2. *Number of visible satellites for a single system.*

Table 3. *Number of visible satellites for a single system.*

Constellation	GPS	GLONASS	BDS	Galileo
Mean number	15.61	10.09	16.92	13.08
Maximum number	20	13	30	17
Minimum number	11	7	10	9
Sample variance	1.64	1.21	15.12	1.52
Mean of location-wise variance	1.63	1.19	15.08	1.51
Mean of the epoch-wise variance	1.63	1.20	3.40	1.52

Afterwards, the number of visible satellites is analysed, and the mean number of visible satellites in the entire GEO belt for the computation period is approximately 15·61 for GPS, 10·09 for GLONASS and 13·08 for Galileo. It indicates that the number of GPS satellites is greater than Galileo, while GLONASS possesses the smallest number, which is related to the total number of satellites of the three constellations in the calculation. With a relatively uniform and symmetrical overall distribution, a greater number of satellites would result in better visibility. In addition, the maximum number and the minimum number of visible satellites for all sampling points in these constellations also conform to this pattern, as shown in Table 3.

The mean number of visible satellites of the BDS is 16·92, which is optimal among the four systems. However, unlike the other constellations, BDS has a maximum of 30 visible satellites, far more than the other three constellations, and a minimum of 10, comparable to the other systems. The difference in the number of visible satellites at different sampling points in the GEO belt is significantly greater for BDS than for the other three systems. The variances of GPS, GLONASS and Galileo are less than 1·64, and variations in the number of visible satellites are not significant. However, the variance of all the sampled values of the BDS is approximately 15·12. The mean of the epoch-wise variance, the variance of the numbers of all longitude samples at each epoch, is only 3·40, whereas the location-wise variance, the variance of the numbers of all epochs at each longitude, is as high as 15·08. This shows that the BDS has significant differences in the number of visible satellites at different longitude positions of the GEO, mainly due to the highly asymmetric configuration of the BDS constellation, which has GEO and

https://doi.org/10.1017/S0373463324000304 Published online by Cambridge University Press

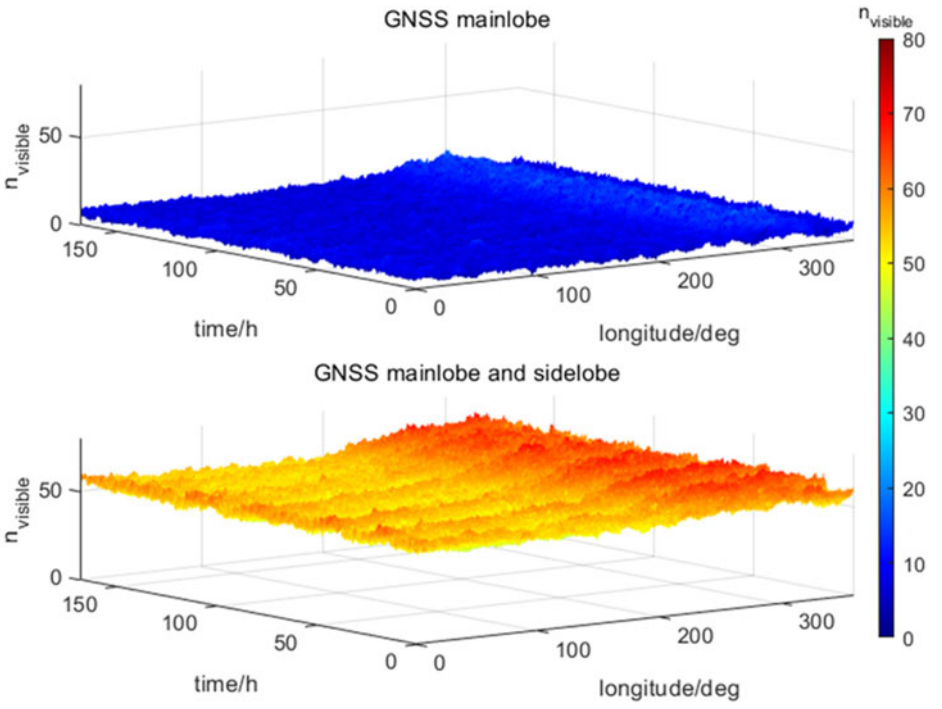


Figure 3. *Number of visible satellites for multi-systems (GNSS).*

IGSO satellites in addition to MEO satellites, compared with the other three constellations that have only MEO satellites. GEO satellites in the ECEF reference frame operate in a fixed region of space that is geostationary with respect to the Earth, whereas IGSO satellites operate within a certain range of longitude and signals would not cover regions outside the corresponding area. This results in fixed coverage of part of the GEO belt by signals from BDS GEO satellites and periodic coverage of part of the GEO belt by signals from IGSO satellites. In turn, this reveals that some GEO regions in the ECEF reference frame would never be able to receive signals from BDS GEO and IGSO satellites, resulting in a phenomenon where there is a significant difference in the number of visible satellites in different longitudes. If only MEO satellites are considered, the variance of all sampled data for BDS is only 2·14, which is not significantly different from the other three systems.

Then considering the visibility of multi-GNSS systems, when receiving signals from four systems at the same time, the number of visible satellites in the GEO belt averages 55·69, with a minimum of 42 and a maximum of 72, which greatly improves the overall navigation performance, as shown in Figure 3. Additionally, if only the main lobe signal is considered, the number of visible satellites is small, with an average of 7·51, a minimum of 0 and a maximum of 21. The performance is worse than when the side lobe is considered, and there are even some scenarios where real-time single-point navigation is not possible, which confirms that considering the side lobe could greatly improve the performance of SSV.

For particular GEO longitudes in the ECEF reference frame, the mean and minimum values of visibility are two important evaluation metrics, as shown in Figure 4. Real-time positioning could be achieved for any system with a minimum number of visible satellites greater than four at any longitude all the time in the GEO belt. An analysis of the overall visibility indicates that GPS outperforms Galileo and GLONASS, while BDS is worse than GPS in the longitude range from 12·2° to 194·2°, but better than GPS in the other ranges. When only the MEO satellites of BDS are considered, the average visibility of BDS is only 13·60, which is slightly better than Galileo. For the area covered by signals of BDS GEO and IGSO satellites, the average number of visible satellites is approximately 18·55, which is 4 higher than that of the uncovered area, and it is even more than 20 satellites stably in the interval from 242·8°

https://doi.org/10.1017/S0373463324000304 Published online by Cambridge University Press

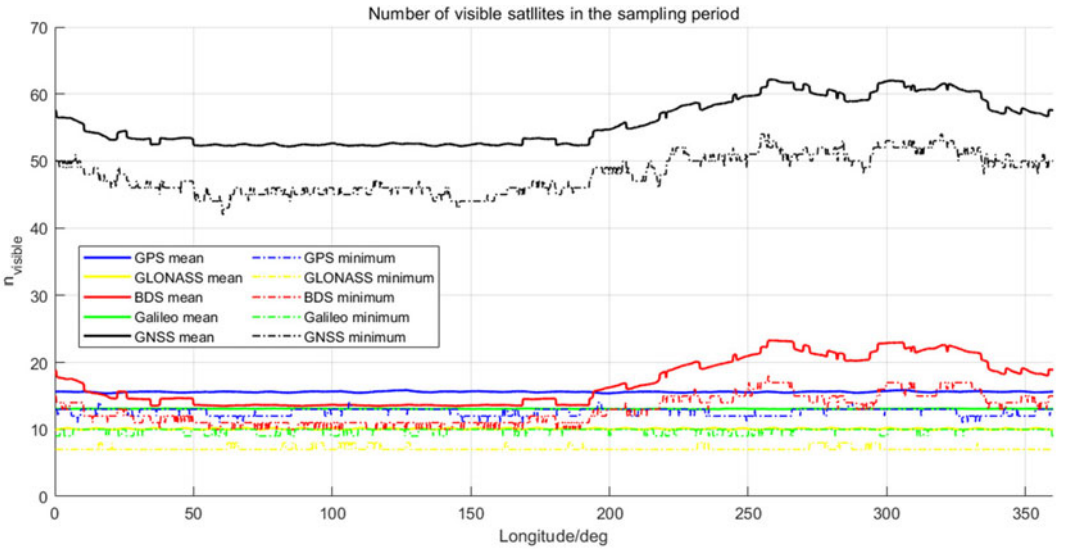


Figure 4. *Average number and minimum number of visible satellites at different longitudes for each system in the ECEF reference frame.*

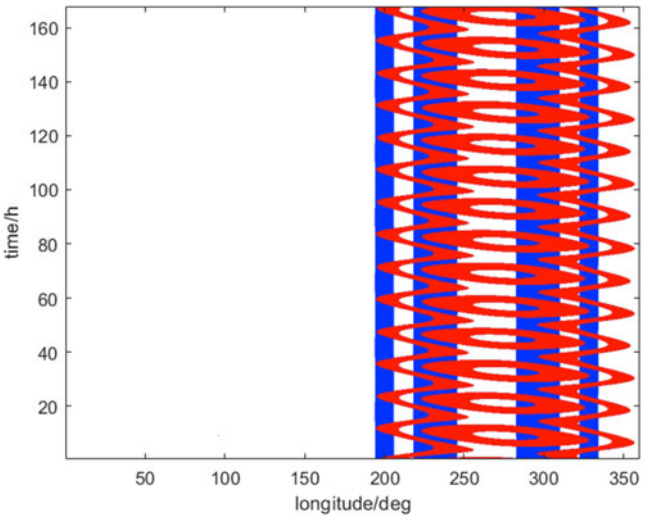


Figure 5. *Signal coverage of a GEO (blue) satellite and an IGSO (red) satellite in the GEO belt.*

to 336·4°, which is much better than that of GPS. In particular, in the area covered by signals from GEO and IGSO satellites, the line of BDS is not smooth compared with the area covered by signals from MEO satellites only, not only because the number of GEO and IGSO satellites is less than MEO satellites, but also because of the narrow range of the available signals from GEO and IGSO satellites.

It is worth noting that GEO satellites are stationary in the ECEF reference frame, while the position of the IGSO satellites is changing, so the different contributions of these two types of satellites to the visibility in the GEO belt have also been investigated. The satellites numbered PRN:C02 (a BDS GEO satellite, hereinafter collectively referred to as "C02") and PRN:C09 (a BDS IGSO satellite, hereinafter collectively referred to as "C09") are selected as an example, and the coverage in the GEO belt by these two satellites during the sampling time period is shown in Figure 5, where the blue and red colours represent that C02 is visible and C09 is visible, respectively.

https://doi.org/10.1017/S0373463324000304 Published online by Cambridge University Press

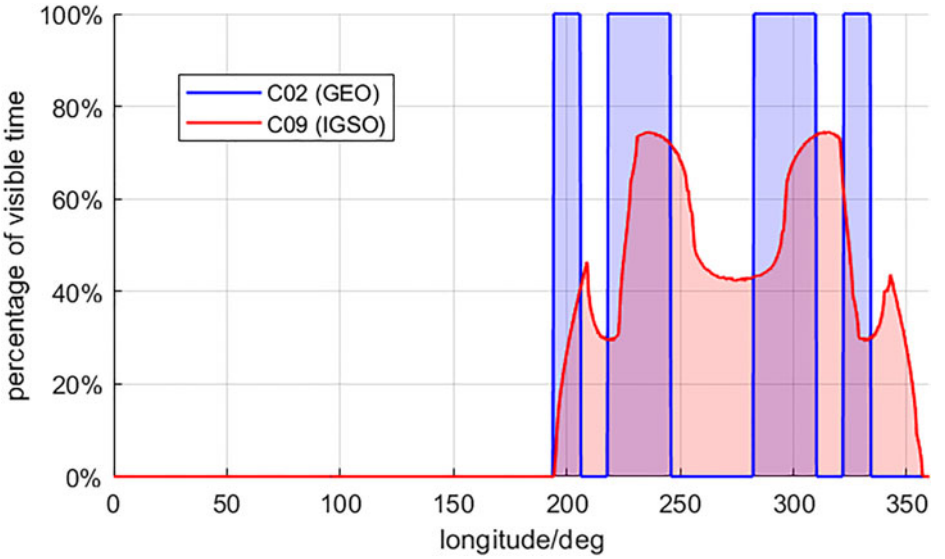


Figure 6. *Percentage of visible time for a GEO satellite and an IGSO satellite in the GEO belt.*

It can be found that the signal of C02 provides permanent coverage of the longitude intervals [194·2, 205·8], [218·2, 245·6], [282·6, 309·8] and [322·2, 333·8] (°), while the signal of C09 provides intermittent coverage of the range from 194·4° to 357°. The percentage of visible time in the GEO belt is shown in Figure 6, where blue and red represent C02 and C09, respectively. It shows that the signal from IGSO satellites has approximately twice the coverage compared with the signal from GEO satellites. However, the permanent coverage by the signal from IGSO satellites cannot be achieved for any location, and the highest percentage is less than 80%.

3.3. PDOP analysis

After completing the visibility analysis, it is then possible to calculate the PDOP of each system for different locations in the GEO belt during the sampling period considering both main lobe and side lobe signals, as shown in Figure 7, noting that GLONASS' *y*-axis is truncated for a better display. Similar to the visibility analysis, the results considering only the main lobe signal are not shown in the figure. The PDOP for all the sampling points of GPS, GLONASS and Galileo are 6·72, 10·11 and 5·71, respectively, as shown in Table 4. It is generally believed that a PDOP of less than 6 yields a better navigation result, but the mean PDOP of GPS and GLONASS for GEO users is greater than 6, resulting in unsatisfactory performance. Galileo has a better result than GPS or GLONASS in terms of mean PDOP, but the value is only 0·29 lower than 6. In particular, ground users located at the equator have a PDOP below 2·4 in the case of using GPS only (Wang et al., 2002), while GEO users have worse positioning results. The main cause of suboptimal results is that navigation satellites serving the GEO satellite are all located on the opposite side of the earth. The excessive radial distance relative to the GNSS constellations' altitudes makes the spatial distribution of the visible satellites relative to the users more concentrated, resulting in a worse PDOP compared with the ground. In addition, the PDOP of each system is correlated with the number of visible satellites, with more visible satellites generally implying better PDOP and resulting in smaller positioning errors. However, since the GEO is above the MEO, the GNSS constellation orbital altitude would make the spatial distribution of satellites relative to the user more centralised, thus making navigation less effective. Results for GLONASS are not only due to the small number of satellites, but also the low orbital altitude, so the PDOP is significantly higher than that of other systems, and the peak value even reaches 48·56, which is the worst overall positioning effect. Galileo has fewer satellites than GPS, but it has the highest orbital altitude among the four systems, resulting in a better performance than GPS.

https://doi.org/10.1017/S0373463324000304 Published online by Cambridge University Press

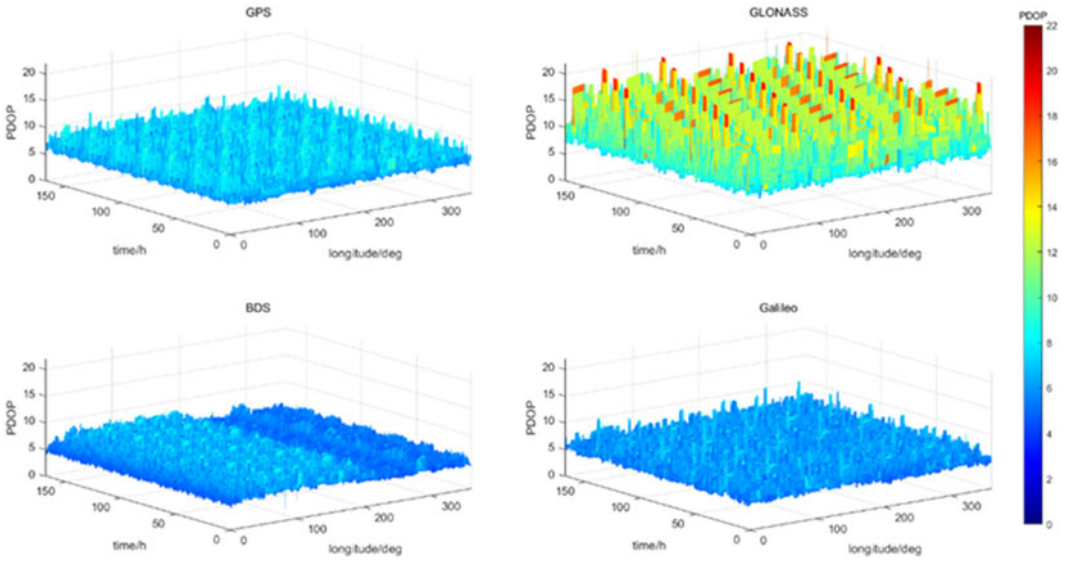


Figure 7. *PDOP for a single system.*

Table 4. *PDOP for a single system.*

Constellation	GPS	GLONASS	BDS	Galileo
Mean PDOP	6.72	10.11	5.69	5.71
Optimal PDOP	4.60	6.25	1.35	3.78
Worst PDOP	13.61	48.56	10.34	12.96

For BDS, the mean value of all sampling points is 5·69, which is better than the other three systems. In particular, similar to the number of visible satellites, the BDS has significant regional differences along the longitude direction. Considering only MEO satellites, BDS has a mean PDOP of 6·40, inferior to Galileo and slightly better than GPS. In the area covered by BDS signals of GEO and IGSO satellites, the mean PDOP is 5·34, which is better than the other three systems. It is mainly because signal coverage from GEO and IGSO satellites effectively increases the number of visible satellites, resulting in a significantly better PDOP for the users located in these areas.

The PDOP for the combination of four systems is shown in Figure 8. If the signals from the four systems are received simultaneously, a mean PDOP of 3·03 can be achieved, and the worst PDOP is less than 4·29, which enables good positioning and argues for the feasibility of SSV in the GEO space using the side lobe signals. The PDOP of the multi-systems considering only the main lobe is also shown. It can be found that the values of PDOP are very high, and there are a large number of sampling points with values exceeding 100, which cannot satisfy the actual navigation requirements at all. The reason for this phenomenon is that main lobe off-boresight angles are too narrow and a large number of signals are obscured by the Earth, which prevents effective service to the GEO belt even with more than 100 navigation satellites.

Specific longitude positions in the ECEF reference frame are analysed next. In practical applications, the evaluation of PDOP needs to consider not only the mean value but also the effect of the vast majority of states. We set the sample space consisting of all the sampling points under a certain longitude and define the random variable of the GEO satellite located at a specific longitude to perform the positioning solution at the moment t as PDOP_t. In this paper, 95% Value at Risk (VaR) will be defined to assess the

https://doi.org/10.1017/S0373463324000304 Published online by Cambridge University Press

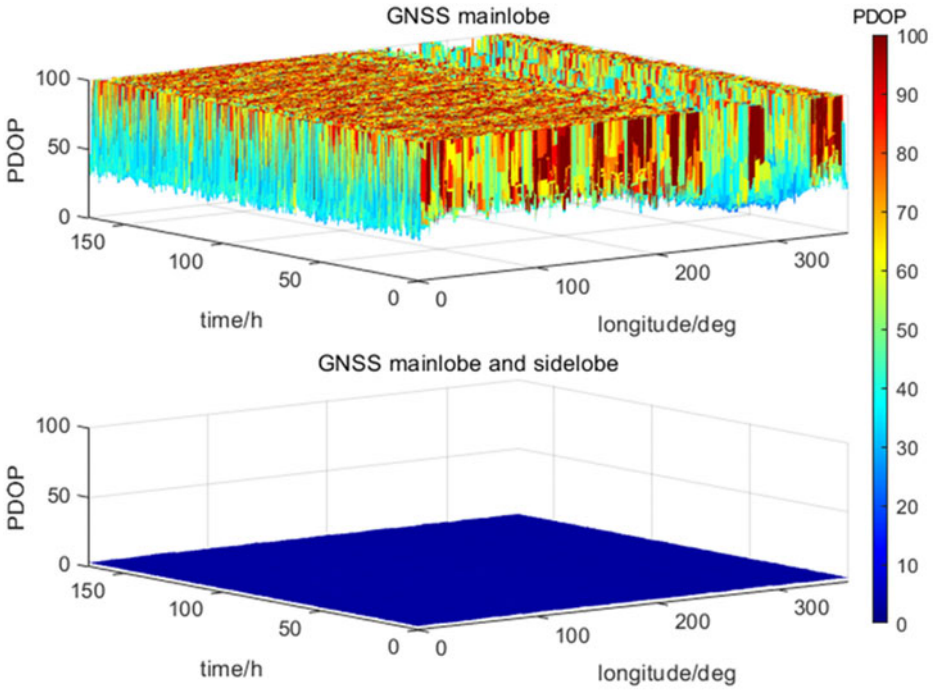


Figure 8. *PDOP for multi-systems.*

effectiveness of different systems for positioning at specific longitude locations, as follows:

$$VaR_{95\%}(\mathrm{PDOP}_t) = \inf\{x | P(\mathrm{PDOP}_t > x) \leq 5\%\} \tag{8}$$

The mean PDOP and $VaR_{95\%}$ for each system at different longitudes are shown in Figure 9. The mean $VaR_{95\%}$ for GPS, GLONASS, BDS and Galileo are 8·28, 13·78, 7·02 and 7·15, respectively, and the mean probability of a PDOP lower than 6 are 21·1%, 0%, 66·8% and 71·1%, respectively, as shown in Table 5. BDS and Galileo have relatively better capabilities but are still unable to achieve a full-time PDOP of less than 6. GPS is slightly less capable, and GLONASS is even not able to achieve positioning with a PDOP of less than 6 at any time. Overall, the PDOP of single-point positioning is unsatisfactory in most cases, and in practical applications, it is necessary to consider a priori information such as orbital dynamics to correct the solution to meet the requirements.

Comparing the overall levels of the different systems, Galileo outperforms GPS and GLONASS. The mean PDOP and $VaR_{95\%}$ of BDS are essentially worse than those of Galileo in the longitude range from 14·6° to 194°, but better than those of Galileo in the other longitude ranges. This is also a result of the fact that the signals from BDS GEO and IGSO satellites in the ECEF reference frame only cover some of the GEO space, and it can be found that the mean $VaR_{95\%}$ of the BDS is also lower than that of Galileo in most of the longitude ranges covered by signals from GEO and IGSO satellites. However, the advantage of BDS in the signal coverage area of GEO and IGSO satellites is not obvious, and the mean PDOP is only less than 0·4 lower than that of Galileo, which is because the PDOP not only put requirements on the visibility but also requires that the geometrical configuration of the visible satellites is conducive to the reduction of errors. Due to the narrow range of the available signals from the GEO and IGSO satellites of BDS, and the small number of satellites, it is difficult to satisfy the requirements of visibility and geometrical configuration at the same time, which improves the PDOP with limited effect. In particular, the reason for the rapid change in the PDOP gradient of the BDS along the longitude direction is similar to that of visibility due to the effect of the fixed coverage area of signals from GEO satellites, but since the PDOP is also affected by the geometrical configuration of the visible

https://doi.org/10.1017/S0373463324000304 Published online by Cambridge University Press

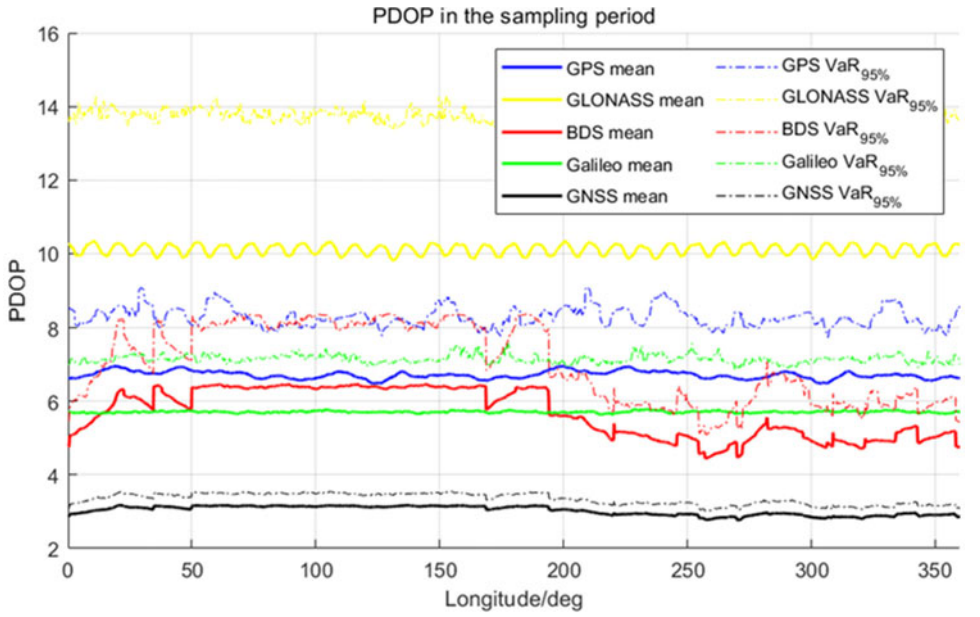


Figure 9. *Mean PDOP and $VaR_{95\%}$ for each system at different longitudes in the ECEF reference frame.*

Table 5. *Overall positioning level for each system.*

Constellation	GPS	GLONASS	BDS	Galileo
Mean $VaR_{95\%}$	8.28	13.78	7.02	7.15
Mean $P\{\text{PDOP}_t < 6\}$	21.1%	0%	66.8%	71.1%

satellites, the effect caused by visibility is relatively attenuated. Overall, the constellation-related results are evaluated, with BDS being the best, Galileo next, GPS slightly worse and GLONASS the worst. The combination of the four systems can realise a PDOP of less than 6 at any time, which is very conducive to the GEO satellite to carry out on-orbit real-time autonomous navigation.

The improvement of PDOP by a single GEO or IGSO satellite is also investigated. Still taking C02 (a BDS GEO satellite) and C09 (a BDS IGSO satellite) as an example, the PDOP result of BDS for the three scenarios of MEO only, MEO + C02 and MEO + C09 is shown in Figure 10. The GEO signal is shown to have a more pronounced improvement in PDOP at some locations, while the IGSO signal has an improvement in PDOP over a wider region. This phenomenon is related to the difference of characteristics in visibility that the GEO signal provides permanent coverage for a smaller region while the IGSO signal provides intermittent coverage for a larger region. Notably, the improvement in PDOP from the GEO signal varies significantly across longitudes, with better improvement in areas near (245·6° and 282·6° for C02) and far (194·2° and 333·8° for C02) from the beam centre. It is mainly because GEO satellites can be more effective in optimising the geometry of the MEO constellation with respect to the users in these regions. For some locations in the range from the Earth-blocked angle and the upper bound of the side lobe, the orientation of GEO satellites with respect to the user is homogenised with the MEO constellation, resulting in a poor improvement of PDOP.

3.4. Validity check through comparison with in-flight data

To verify the validity and reasonableness of the result, measured data from three GEO missions at fixed longitude were selected and compared with the result of this study (Winkler et al., 2017; Wang et al.,

https://doi.org/10.1017/S0373463324000304 Published online by Cambridge University Press

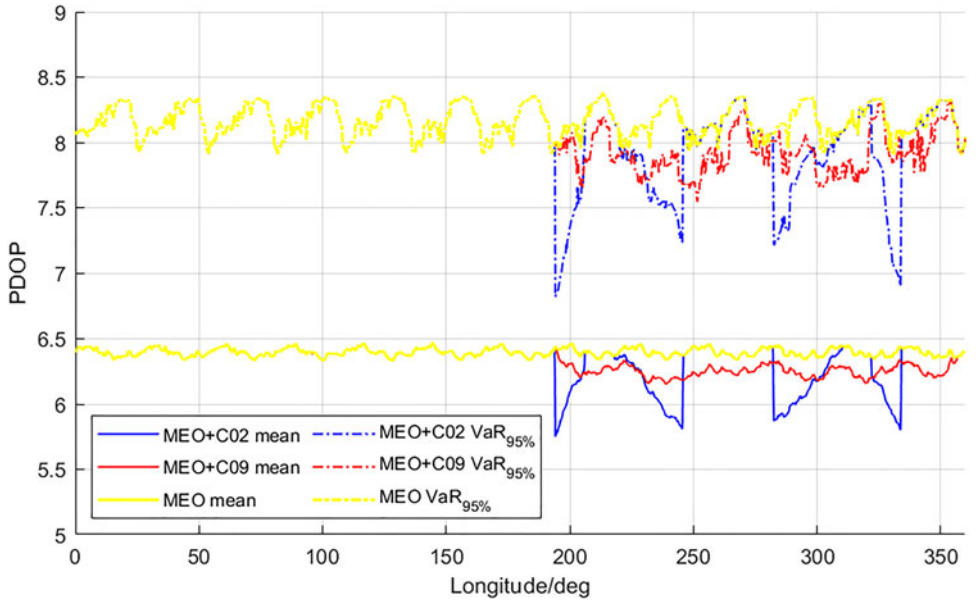


Figure 10. *Differences between a GEO satellite and an IGSO satellite in the improvement of PDOP for BDS.*

Table 6. *Validation of results against measured data from several missions.*

Mission	GOES-R	TJS-2	JDRS-1
Longitude of GEO (°)	284.8	107.4	90.8
Mean number of tracked navigation satellites from measured data	11.1	7.6	8
Mean PDOP from measured data	7.9	10.8	[a]
Mean PDOP in this study	6.7	6.8	6.6

[a]The data recorded for JDRS-1 are in the form of mean GDOP, mainly distributed between 8·3 and 16·7, with some sampling points exceeding 50, which is not reasonable for calculating the mean number.

2021; Nakajima et al., 2023), as shown in Table 6. The first case was the GOES-R launched by the United States in 2016, with data from February 2nd to 4th, 2017. The second case was the TJS-2 launched by China in 2017, with data from February 16th to 19th, 2017. Finally, the third case was the JDRS-1 launched by Japan in 2020, with data from January 10th to 14th, 2021. All of them were equipped with GPS weak signal receivers that enabled the reception of side lobe signals, and the average number of tracked navigation satellites for the measured data was 11·1, 7·6 and 8, respectively. Moreover, the measured data of mean PDOP indicates the validity of this study. It is worth noting that the discrepancy between measured and theoretical values does exist, but this gap is reasonable. Because the measured values may vary to some extent due to the difference in selected periods, the different operational status of the GNSS constellations and the different number of navigation satellites in a healthy state. Furthermore, different manufacturers have different levels of receiver design and manufacturing, so the effect of the terminal on the level of positioning varies significantly. In this paper, the precise ephemeris was used, and the user side was set as the ideal state, so theoretical values would be better than the measured value. Additionally, there is a difference between the definitions of 'visible' and 'tracked', where 'visible' refers to the number of signals covering the GEO satellite, whereas 'tracked' refers to the number of signals processed by the receiver. The number of tracked navigation satellites is affected

https://doi.org/10.1017/S0373463324000304 Published online by Cambridge University Press

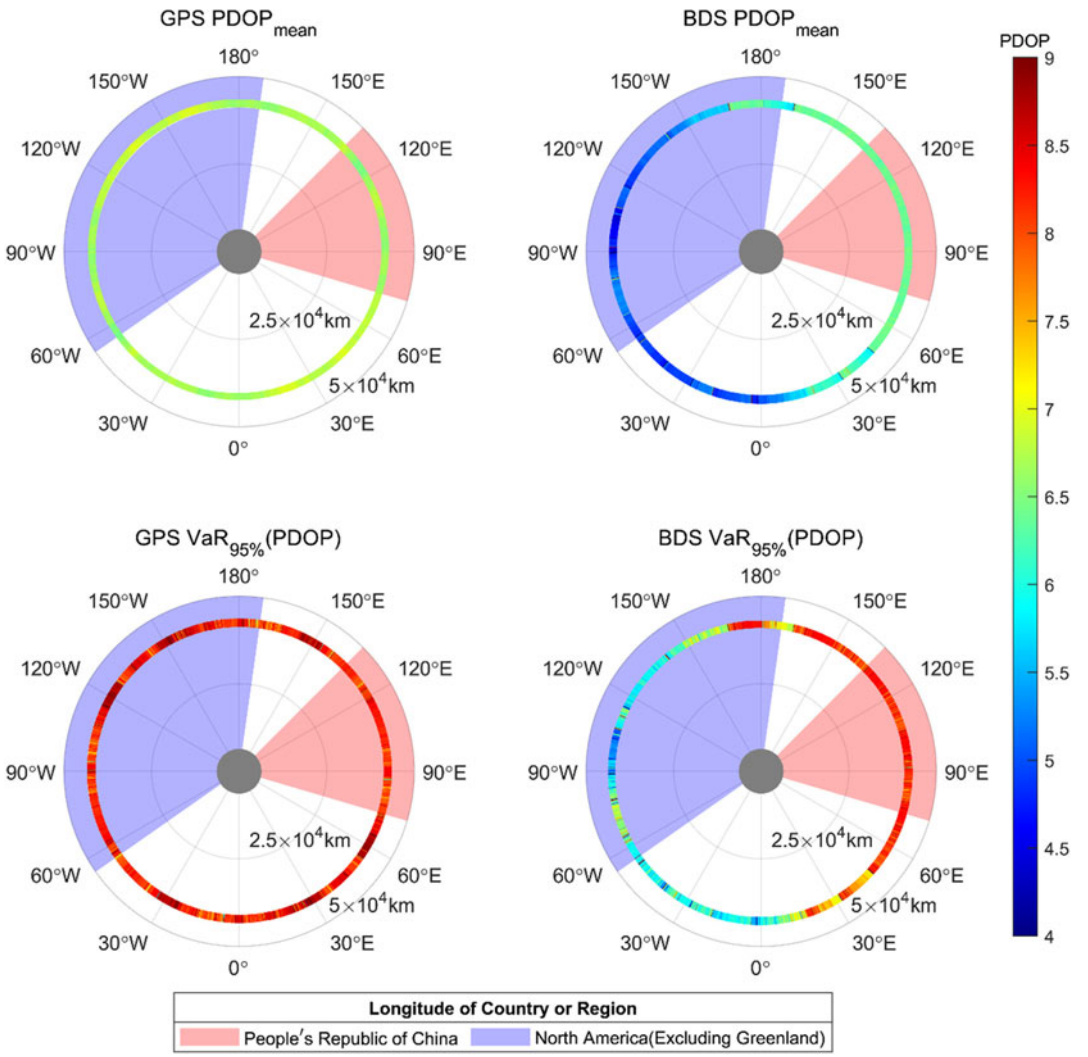


Figure 11. *Positioning capability for GPS and BDS in the GEO belt.*

by receiver sensitivity, channel number and on-board algorithm. Thus, the number of tracked satellites in the three sets of measured data would be significantly smaller than the number of visible satellites of approximately 15 in the calculation.

3.5. Contribution to mission capabilities

For autonomous operations in GEO, a more robust autonomous navigation capability means an advantage in actually executing the mission. General GEO satellites only need to operate in a particular longitude region, and for China, since the determination and other tasks are highly dependent on ground stations, Chinese satellites can only operate in the space visible to ground stations, which is seriously limited by the territorial scope. However, GEO on-orbit servicing satellites need to constantly patrol the GEO belt and perform missions at different GEO longitudes, whereas large infeasible regions for missions exist in the case of Chinese ground station support only. Autonomous navigation using the GNSS space service proposed in this paper could enhance the capability of Chinese GEO users to perform missions in the GEO region beyond the borders. In particular, this paper compares the performance of the most commonly used GPS and BDS, and analyses the autonomous navigation capabilities based on GNSS

https://doi.org/10.1017/S0373463324000304 Published online by Cambridge University Press

systems in the GEO belt, as shown in Figure 11. BDS has a lower mean PDOP than GPS in the entire GEO belt, possessing smaller positioning errors, and this advantage is more pronounced over the Western Hemisphere due to the coverage of signal from GEO and IGSO satellites. In space over China, since the GEO and IGSO satellite signals of BDS cannot effectively cover this area, the autonomous navigation based on BDS could only rely on MEO satellites, and thus the advantage in positioning effects of BDS is not obvious. When the satellite operates in space that is beyond the borders, the mean PDOP and $VaR_{95\%}$ are significantly improved thanks to the coverage of signals from BDS GEO and IGSO satellites. In particular, over North America and the Atlantic Ocean, the mean PDOP of BDS is 5·20, a decrease of 1·52 compared to 6·72 for GPS; and the $VaR_{95\%}$ of BDS is 6·26, a decrease of 2·02 compared to 8·28 for GPS. Further, over these regions, BDS can realise the requirement of high accuracy with a PDOP of less than 6 during 87·2% of the time, which is significantly better than 21·0% of GPS. Thus, using BDS for navigation is conducive to the tasks carried out by GEO on-orbit servicing satellites.

4. Conclusion

This paper investigated the autonomous navigation scheme of GEO users based on the GNSS space service. It evaluated the key parameters affecting positioning capability, analysed the number of visible satellites and evaluated values of PDOP across different satellite navigation systems in the GEO belt. The following conclusions have been drawn.

1) Considering the side lobe signal, the average number of visible satellites in the GEO belt for GPS, GLONASS, BDS and Galileo stands at 15·61, 10·09, 16·92 and 13·08, respectively. Notably, the minimum number of visible satellites for all systems is greater than 4, meeting the requirement for providing single-point real-time positioning for the users across all longitude positions in GEO. BDS exhibits consistent visibility of over 20 satellites in the 242·8° to 336·4° interval of the GEO belt, attributed to the constellation of mixed GEO/IGSO/MEO satellites. Overall, BDS outperforms GPS, which, in turn, outperforms Galileo and GLONASS in terms of visibility. The cumulative number of visible satellites using a combination of these four systems reaches an impressive 55·69 on average. In addition, the signal from IGSO satellites has approximately twice the coverage compared to the signal from GEO satellites, but permanent coverage by IGSO signals cannot be achieved for any location.
2) Considering side lobe signals, the mean PDOP for the GEO belt is 6·72 for GPS, 10·11 for GLONASS, 5·69 for BDS and 5·71 for Galileo. Notably, BDS holds an advantage in the area covered by signals of GEO and IGSO satellites, resulting in a mean PDOP of 5·34. In an overall evaluation of the positioning effect of each system, BDS outperforms GPS, which, in turn, outperforms Galileo and GLONASS. When combining all four systems, the mean PDOP is 3·03, consistently meeting the demand for high-precision positioning with a PDOP of less than 6 at all times. In particular, GEO signals have a more pronounced improvement in PDOP at some locations, while the IGSO signals have an improvement in PDOP over a wider region.
3) China's operational range for GEO satellites is constrained by the distribution of ground stations. However, GEO users can leverage GNSS signals for autonomous navigation beyond these borders. In addition, thanks to the sustained and stable signal coverage from BDS GEO and IGSO satellites on the opposite side of the earth, the mean PDOP and $VaR_{95\%}$ of BDS are 5·20 and 6·26 for GEO users over North America and the Atlantic Ocean, while the corresponding values of GPS are 6·72 and 8·28, respectively. In addition, over these regions, BDS can meet the high-precision requirement of a PDOP less than 6 during 87·2% of the time, presenting a notable improvement compared with 21·0% of GPS.

Availability of data and material. The ephemeris can be accessed at http://www.igmas.org/Product/Search/index/cate_id/38.html. The datasets used and/or analysed during the current study are available from the corresponding author upon reasonable request.

https://doi.org/10.1017/S0373463324000304 Published online by Cambridge University Press

Acknowledgment. We thank the iGMAS for the high-quality ephemeris data and products. In addition, the authors gratefully acknowledge Gang Wang (Academy of Space Information Systems) for providing design parameters about navigation satellite transmitters considering SSV and Wenhai Jiao (Beijing Institute of Tracking and Telecommunications Technology) for his useful comments and suggestions on paper structure.

Authors' contributions. F.J. proposed the idea and carried out the experiment; X.Y. assisted in carrying out the experiment; F.J. drafted the paper; Y.H. revised the paper. All authors read and approved the final manuscript.

Funding. Not applicable.

Competing interests. All authors declare that there are no other competing interests.

References

Ananda, M. P. and Jorgensen, P. S. (1985). Orbit Determination of Geostationary Satellites Using the Global Positioning System. In *Proceedings of the Symposium on Space Dynamics for Geostationary Satellites*, Toulouse, France.

Ashman, B., Bauer, F. H., Parker, J. and Donaldson, J. (2018). GPS Operations in High Earth Orbit: Recent Experiences and Future Opportunities. In *Proceedings of the 15th International Conference on Space Operations (SpaceOps 2018)*, Marseille, France.

Barker, L. and Frey, C. (2012). GPS at GEO: A First look at GPS From SBIRS GEO1. In *Proceedings of the 35th Annual AAS Guidance and Control Conference*, Breckenridge, Colorado.

Bauer, F. H., Moreau, M. C., Dahle-Melsaether, M. E., Petrofski, W. P., Stanton, B. J., Thomason, S., Harris, G. A., Sena, R. P. and Temple, L. P. III. (2006). The GPS Space Service Volume. In *Proceedings of the 19th International Technical Meeting of the Satellite Division of the Institute of Navigation (ION GNSS 2006)*, Fort Worth, Texas.

Bauer, F. H., Parker, J. J. K., Welch, B. and Enderle, W. (2017). Developing A Robust, Interoperable GNSS Space Service Volume (SSV) for the Global Space User Community. In *Proceedings of the 2017 International Technical Meeting of The Institute of Navigation*, Monterey, California.

Bock, H., Hugentobler, U., Springer, T. A. and Beutler, G. (2002). Efficient precise orbit determination of LEO satellites using GPS. *Advances in Space Research*, **30**(2), 295–300. doi:10.1016/s0273-1177(02)00298-3

Capuano, V., Shehaj, E., Blunt, P., Botteron, C. and Farine, P. A. (2017). High accuracy GNSS based navigation in GEO. *Acta Astronautica*, **136**, 332–341. doi:10.1016/j.actaastro.2017.03.014

Chai, J., Wang, X., Yu, N., Wang, D. and Li, Q. (2018). Modeling and intensity analysis of GNSS signal link for high-orbit spacecraft. *Journal of Beijing University of Aeronautics and Astronautics*, **44**(7), 1496–1503. doi:10.13700/j.bh.1001-5965.2017.0502

Combined Force Space Component Command (2023). Space-track. https://www.space-track.org/#/favorites (accessed 21 September 2023).

Du, L. (2006). A study on the precise orbit determination of geostationary satellites. Doctoral dissertation, Information Engineering University.

Filippi, H., Gottzein, E., Kuehl, C., Mueller, C., Barrios-Montalvo, A. and Dauphin, H. (2010). Feasibility of GNSS Receivers for Satellite Navigation in GEO and Higher Altitudes. In *2010 5th ESA Workshop on Satellite Navigation Technologies and European Workshop on GNSS Signals and Signal Processing (NAVITEC)*, Noordwijk, Netherlands.

Guan, M., Xu, T., Li, M., Gao, F. and Mu, D. (2022). Navigation in GEO, HEO, and Lunar trajectory using multi-GNSS sidelobe signals. *Remote Sensing*, **14**(2), 318. doi:10.3390/rs14020318

Jiang, K., Li, M., Wang, M., Zhao, Q. and Li, W. (2018). TJS-2 geostationary satellite orbit determination using onboard GPS measurements. *GPS Solutions*, **22**(3), 87. doi:10.1007/s10291-018-0750-x

Jing, S., Zhan, X., Lu, J., Feng, S. and Ochieng, W. (2015). Characterisation of GNSS space service volume. *The Journal of Navigation*, **68**(1), 107–125. doi:10.1017/S0373463314000472

Kang, Z., Tapley, B., Bettadpur, S., Ries, J., Nagel, P. and Pastor, R. (2006). Precise orbit determination for the GRACE mission using only GPS data. *Journal of Geodesy*, **80**(6), 322–331. doi:10.1007/s00190-006-0073-5

Li, M., Li, W., Shi, C., Jiang, K., Guo, X., Dai, X., Meng, X., Yang, Z., Yang, G. and Liao, M. (2017). Precise orbit determination of the Fengyun-3C satellite using onboard GPS and BDS observations. *Journal of Geodesy*, **91**(11), 1313–1327. doi:10.1007/s00190-017-1027-9

Lin, K., Zhan, X., Yang, R., Shao, F. and Huang, J. (2020). BDS space service volume characterizations considering side-lobe signals and 3D antenna pattern. *Aerospace Science and Technology*, **106**, 106071. doi:10.1016/j.ast.2020.106071

Lorga, J. F. M., Silva, P. F., Dovis, F., Di Cintio, A., Kowaltschek, S., Jimenez, D. and Jansson, R. (2010). Autonomous Orbit Determination for Future GEO and HEO Missions. In *2010 5th ESA Workshop on Satellite Navigation Technologies and European Workshop on GNSS Signals and Signal Processing (NAVITEC)*, Noordwijk, Netherlands.

Maestrini, M. and Di Lizia, P. (2022). Guidance strategy for autonomous inspection of unknown non-cooperative resident space objects. *Journal of Guidance, Control, and Dynamics*, **45**(6), 1126–1136. doi:10.2514/1.g006126

Marmet, F. X., Maureau, J., Calaprice, M. and Aguttes, J. P. (2015). GPS/Galileo navigation in GTO/GEO orbit. *Acta Astronautica*, **117**, 263–276. doi:10.1016/j.actaastro.2015.08.008

https://doi.org/10.1017/S0373463324000304 Published online by Cambridge University Press

Marquis, W. A. and Reigh, D. L. (2015). The GPS block IIR and IIR-M broadcast L-band antenna panel: Its pattern and performance. *NAVIGATION: Journal of the Institute of Navigation*, **62**(4), 329–347. doi:10.1002/navi.123

Meng, L., Wang, J., Chen, J., Wang, B. and Zhang, Y. (2020). Extended geometry and probability model for GNSS+ constellation performance evaluation. *Remote Sensing*, **12**(16), 2560. doi:10.3390/rs12162560

Nakajima, Y., Yamamoto, T., Miyashita, N., Shintate, K., Matsumoto, T., Sakamoto, T., Harada, R. and Kumagai, S. (2023). Flight results of GPS receiver for geosynchronous satellites. *Journal of Evolving Space Activities*, **1**, 24. doi:10.57350/jesa.24

Qin, H. and Liang, M. (2008). Research on positioning of high earth orbital satellite using GNSS. *Chinese Journal of Space Science*, **28**(4), 316–325. doi:10.11728/cjss2008.04.316

Shi, T., Zhuang, X. and Xie, L. (2021). Performance evaluation of multi-GNSSs navigation in super synchronous transfer orbit and geostationary earth orbit. *Satellite Navigation*, **2**(1), 5. doi:10.1186/s43020-021-00036-0

Starek, J. A., Açıkmeşe, B., Nesnas, I. A. and Pavone, M. (2016). Spacecraft autonomy challenges for next-generation space missions. In: Feron, E. (ed.). *Advances in Control System Technology for Aerospace Applications*, Berlin, Heidelberg: Springer, 1–48.

Union of Concerned Scientists. (2023). UCS satellite database. https://www.ucsusa.org/resources/satellite-database#.W7WcwpMza9Y (accessed 21 September 2023).

United Nations Office for Outer Space Affairs. (2021). *The Interoperable Global Navigation Satellite Systems Space Service Volume* (2nd ed). Vienna: United Nations Office.

Wang, J., Iz, B. and Lu, C. (2002). Dependency of GPS positioning precision on station location. *GPS Solutions*, **6**(1), 91–95. doi:10.1007/s10291-002-0021-7

Wang, W., Dong, X., Liu, L. and Yang, Y. (2011). Research and simulation of orbit determination for geostationary satellite based on GNSS. *Acta Geodaetica et Cartographica Sinica*, **40**(Sup.), 6–10.

Wang, M., Wang, J., Dong, D., Meng, L., Chen, J., Wang, A. and Cui, H. (2019). Performance of BDS-3: Satellite visibility and dilution of precision. *GPS Solutions*, **23**(2), 56. doi:10.1007/s10291-019-0847-x

Wang, M., Shan, T. and Wang, D. (2020). Development of GNSS technology for high earth orbit spacecraft. *Acta Geodaetica et Cartographica Sinica*, **49**(9), 1158–1167. doi:10.11947/j.AGCS.2020.20200170

Wang, M., Shan, T., Li, M., Liu, L. and Tao, R. (2021). GNSS-based orbit determination method and flight performance for geostationary satellites. *Journal of Geodesy*, **95**(8), 89. doi:10.1007/s00190-021-01545-1

Weeden, B. and Samson, V. (2018). *Global Counterspace Capabilities: An Open Source Assessment*. Washington, D.C.: Secure World Foundation.

Winkler, S., Ramsey, G., Frey, C., Chapel, J., Chu, D., Freesland, D., Krimchansky, A. and Concha, M. (2017). GPS Receiver on-Orbit Performance for the GOES-R Spacecraft. In *10th International ESA Conference on Guidance, Navigation and Control Systems*, Salzburg, Austria.

Winternitz, L. M. B., Bamford, W. A. and Heckler, G. W. (2009). A GPS receiver for high-altitude satellite navigation. *IEEE Journal of Selected Topics in Signal Processing*, **3**(4), 541–556. doi:10.1109/JSTSP.2009.2023352

Woffinden, D. C. and Geller, D. K. (2007). Navigating the road to autonomous orbital rendezvous. *Journal of Spacecraft and Rockets*, **44**(4), 898–909. doi:10.2514/1.30734

Xu, W., Liang, B., Li, B. and Xu, Y. (2011). A universal on-orbit servicing system used in the geostationary orbit. *Advances in Space Research*, **48**(1), 95–119. doi:10.1016/j.asr.2011.02.012

Yang, J., Wang, X. and Chen, D. (2021). Design of a GNSS vector tracking scheme for high-orbit space. *Journal of Beijing University of Aeronautics and Astronautics*, **47**(9), 1799–1806. doi:10.13700/j.bh.1001-5965.2020.0300

Zeng, Z., Hu, X., Zhang, X. and Wan, W. (2004). Inversion methods for ionospheric occultation from GPS observation data. *Chinese Journal of Geophysics*, **47**(4), 660–666. doi:10.1002/cjg2.3534

Zhao, X., Zhou, S., Ci, Y., Hu, X., Cao, J., Chang, Z., Tang, C., Guo, D., Guo, K. and Liao, M. (2020). High-precision orbit determination for a LEO nanosatellite using BDS-3. *GPS Solutions*, **24**(4), 102. doi:10.1007/s10291-020-01015-9

Zou, D., Zhang, Q., Cui, Y., Liu, Y., Zhang, J., Cheng, X. and Liu, J. (2019). Orbit determination algorithm and performance analysis of high-orbit spacecraft based on GNSS. *IET Communications*, **13**(20), 3377–3382. doi:10.1049/iet-com.2019.0434

Cite this article: Jiao F, Hu Y, Yu X (2024). Performance of GNSS space service for geostationary autonomous operations. *The Journal of Navigation* **77**: 2, 257–275. https://doi.org/10.1017/S0373463324000304

https://doi.org/10.1017/S0373463324000304 Published online by Cambridge University Press